

New Results of Observations of the Only Supernova Remnant in the IC1613 Galaxy.

Lozinskaya T.A.¹, Podorvanyuk N.Yu.¹

November 8, 2018

¹*Sternberg Astronomical Institute, Universitetskii pr. 13, Moscow, 119992 Russia*

Received 00.00.2008

Abstract

ABSTRACT

The new results of a study of the kinematics of the supernova remnant S8 in the IC1613 galaxy are reported. The expansion velocity of the bright optical nebula is determined based on observations made with the 6-m telescope of the Special Astrophysical Observatory of the Russian Academy of Sciences using MPFS field spectrograph and SCORPIO focal reducer operating in the scanning Fabry–Perot interferometer mode. An analysis of 21-cm line VLA observations of the galaxy corroborates our earlier proposed model of a SN exploding inside a cavern surrounded by a dense shell and S8 colliding with the wall of the HI shell.

1 Introduction

The only known supernova remnant in the Irr galaxy IC1613 — the bright nebula S8 (Sandage, 1971) — resides in a giant complex of multiple ionized shells (Meaburn et al., 1988; Lozinskaya et al., 2001; Lozinskaya et al., 2002) in the Northeastern sector of the galaxy.

Lozinskaya et al. (1998) (hereafter referred to as Paper (I)) showed this remnant to be an x-ray source and observed S8 at optical and radio wavelengths. These observations revealed the peculiar nature of the object, which combines the properties of an old and a young supernova remnant, i.e., high brightness at both optical and x-ray ranges. In Paper (I) we proposed a model where a supernova explodes inside a cavern surrounded by a dense shell and the expanding SNR collides with the wall of this dense shell. In this case, bright optical emission is due to the gas located behind the radiative cooling shock in the dense shell, whereas bright x-ray emission, to the hot plasma behind the shock that propagates in the inner tenuous cavern. Rosado et al. (2001) criticized this model and suggested that half of the remnant in question is simply unobservable because of dust.

We studied the kinematics of ionized and neutral gas in the entire complex of ongoing star formation in the galaxy in an earlier paper (Lozinskaya et al., 2003). In this paper we perform further analysis of the kinematics of the optical supernova remnant based on observations made with the 6-m telescope of the Special Astrophysical Observatory using MPFS spectrograph and focal reducer SCORPIO operating in the scanning Fabry–Perot interferometer mode (Moiseev, 2002), and also search for an extended dense shell or for a dense HI layer based on the results of 21-cm line VLA observations.

In the followings sections we report the results of observations of the supernova remnant made with the MPFS and with SCORPIO operating in the scanning Fabry–Perot interferometer mode, which revealed for the first time the expansion of the bright nebula. The results of VLA observations allowed us to identify the external HI shell, thereby supporting the model that we proposed in Paper (I). In the Conclusions section we summarize the main conclusions of this paper.

All velocities mentioned in this paper are heliocentric, and we assume that the distance to the galaxy is equal to 725–730 kpc (Freedman, 1988).

Table 1. Parameters of the new and old MPFS.

Instrument	Old MPFS	New MPFS
Size of the "micropupil"	1.3"	0.75"
Field of view	10.4"x20.8"	12"x11.25"
CCD	1040x1160 px	1024x1024 px
Wavelength interval	4000 - 7500 Å	5800 - 7180 Å
Dispersion	1.6 Å/px	1.35 Å/px
Spectroscopic resolution	2,5 - 5 Å	3 - 4 Å
Seeing	1.6" - 1.7"	1.1"

2 Structure and Kinematics of the Supernova Remnant According to Observations Made with the 6-m Telescope using MPFS Spectrograph and Fabry–Perot Interferometer

2.1 Observations and Data Reduction

MPFS Observations. In 2001 we performed our observations with the new version of MPFS spectrograph, which was an upgraded version of the instrument employed in Paper I. A description of the spectrograph can be found at

(http://www.sao.ru/hq/lsfvo/devices/mpfs/mpfs_main.html).

Table 1 lists the parameters of two spectrographs. The last row of the table gives the seeing during the 1996 and 2001 observations.

We reduced our observations using the IDL software developed at the Special Astrophysical Observatory of the Russian Academy of Sciences. Primary reduction included bias subtraction, flatfielding, cosmic-ray hit removal, extraction of individual spectra from CCD frames, and wavelength calibration of these spectra using the spectrum of the He-Ne-Ar filled calibration lamp. We then subtracted the night-sky spectrum from the linearized spectra and converted the observed fluxes into absolute energy scale using spectrophotometric standards observed at the same zenith distance as IC 1613.

Interferometric observations in the H α line were made with SCORPIO focal reducer and scanning Fabry–Perot interferometer (FPI). A description of the parameters of the IFP501 interferometer employed and of the reduction technique can be found in the paper by Lozinskaya et al. (2003). The size of the field of view was 4.8' and the image scale was 0.56"/px. The distance between adjacent orders ensured an overlap-free velocity interval from -2 to -584 km/s; the number of spectral channels was 36, and the width of a single channel was $\delta\lambda \approx 0.36\text{\AA}$, i.e., ~ 16 km/s in the radial-velocity scale.

2.2 Brightness Distribution and Velocity Field in the SNR S8

Our observations of the supernova remnant with the new version of MPFS yield HeI (5876 Å), [OI] (6300 Å), [OI] (6364 Å), H α , [NII] (6583 Å), [SII] (6717+6731Å), HeI (7065 Å),

and Fe II (7155 Å) line brightness distribution maps, all of which have similar structure and agree with the results of Paper (I). Figure 1 shows the velocity fields based on the maximum of the contour for each of the spectral lines mentioned above as measured with MPFS spectrograph with the H α -line brightness distribution of the SNR superimposed.

2.3 Kinematics of the SNR S8

In Paper (I) we fitted the H α line profile by a superposition of three Gaussians and identified the following three components: the bright "main" one and two weak components in the line wings at the level of 10-20% of maximum intensity. The latter are the blue and red components shifted by (-150 \div - 423 km/s) and (145 \div 295 km/s), respectively, with respect to the main component. The main component of the H α line shows a velocity gradient from -340 km/s in the Western part to -290 km/s in the Eastern part (see Fig. 6 in Paper (I)).

A reduction of our new MPFS observations made with superior resolution and seeing compared to those published in Paper (I) yielded the optimum fit to the H α line in the form of two bright components – the red component at about -240 km/s and the blue one whose velocity differs from that of the red component by up to -70 km/s. Figure 2 shows examples of the decomposition of the line profile at different locations in the nebula according to MPFS observations.

Our observations made with the scanning FPI are also suggest that the spectral line consists of two bright components — the red and the blue — with almost the same velocities as those inferred from MPDS data. The velocity of the red component is equal to about -240 km/s, whereas that of the blue component is offset to within -100 km/s. Figure 3 illustrates the decomposition of the line profile obtained with the FPI.

In both series of observations the two components have comparable intensities. Note that we do not discard the weak components in the line wings found in Paper (I). FPI and MPFS observations record emission at the level of 10–20% of the maximum intensity in the velocity intervals from -450 to -150 km/s and from -500 to -100 km/s, respectively.

Figures 4a and 4b show the "position-velocity" (P/V) diagrams for MPFS and FPI observations of the two bright components of the H α line, which we use to reveal the expansion of the supernova remnant. We draw three to four P/V diagrams for the directions parallel to the major axis of the remnant for both observational series and P/V diagrams parallel to the minor axis based on the results of FPI observations.

These P/V diagrams reveal the expansion of the S8 nebula. The blue component, which must be produced by the approaching side of the shell, shows a bended P/V diagram (half of the so-called "velocity ellipse"), which is typical of an expanding shell. The expansion velocity of the bright side of the shell as inferred from this bend is equal to 75 \pm 25 km/s.

The average velocity of the "unshifted" component of ionized gas emission in the neighborhood of the supernova remnant as inferred from FPI observations is equal to -240 \div -256 km/s, which is consistent with earlier observations by Lozinskaya et al. (1998) and Rosado et al. (2001). According to the results of the decomposition of the H α line, the second, red component shows similar velocities. Given that inside the remnant this component has higher intensity than the "unshifted" component of the emission of gas outside the remnant, we assume that it must result from a superposition of the emission

of the receding side of the shell and that of unperturbed gas along the line of sight.

3 Extended Outer Shell in the Neighborhood of the SNR

The results of our detailed analysis of the HI kinematics in the IC 1613 galaxy based on 21-cm line VLA observations can be found in our earlier papers (Lozinskaya et al., 2003; Silich et al., 2006).

Figure 5 shows the 21-cm line VLA image of the galaxy region we are interested in with $H\alpha$ brightness isophotes superimposed. The arrow points to the supernova remnant. We computed the HI brightness distribution map by integrating archive VLA data over 40 channels out of 127 (in the velocity interval from -279 to -178 km/s), because no 21-cm line emission was recorded from the galaxy in the remaining channels. We computed the monochromatic $H\alpha$ image by integrating the flux in this line in the spectra taken with the FPI.

We find the mean HI velocity in the region of the star-forming complex as inferred from the emission of "unaccelerated" gas recorded in all scans to be $V_{HI} = -230 \pm 5$ km/s, which is quite consistent with the estimate of Lake and Skillman (1989) for this part of the galaxy based on low angular resolution observations.

It follows from Fig. 5 that the supernova remnant is located at the outer boundary of the densest HI layer in the galaxy, which on the South borders shell II (according to the naming convention of Lozinskaya et al., 2003). The bright shell II is bordered on the South by another faint neutral shell with the supernova remnant residing at its inner boundary. Our P/V diagrams shows signs of the expansion of this neutral shell — see scan 1 (positions 33 - 63 arcec), scan 2 (90 - 130 arcsec), and scan 3 (60 - 77 arcsec) in Fig 5.

We already mentioned one of these diagrams in our earlier paper (Lozinskaya et al., 2003) as evidence supporting the model discussed. The remnant resides at the inner boundary of the shell and its location in the P/V diagrams in Fig. 5 is indicated by the arrow. The expansion velocity of the matter in the wall of the HI shell in the region of the remnant is greater than 10 km/s.

4 Discussion

We performed a detailed study of the kinematics of the bright nebula — the SNR S8 — with both MPFS spectrograph and scanning FPI attached to the 6-m telescope of the Special Astrophysical Observatory of the Russian Academy of Sciences. We identified two bright components in the $H\alpha$ line profile without discarding the weak red and blue components in the wings of this line found in Paper (I).

Our "position-velocity" diagrams revealed for the first time the effect of the expansion of the bright optical supernova remnant S8 with a velocity of 75 ± 25 km/s.

The inferred expansion velocity suggests that bright optical emission of the remnant is indeed due to the gas located behind the radiative cooling shock. In Paper I we made this conclusion based solely on the high brightness of optical radiation.

Note that the expansion velocity inferred from the maximum of the line characterizes the average velocity of the brightest features; fainter emission is observed over a wide velocity interval spanning from -500 to -50 km/s. This is a typical situation in all thoroughly studied bright optical supernova remnants, which is due to the nonuniform density distribution in the ambient medium. Different cloudlets through which the radiative-cooling shock propagates differ in density, stages of interaction with the shock, and in their orientation with respect to the observer.

We used 21-cm line VLA observations to identify the extended neutral shell at whose inner boundary the supernova remnant resides. We also revealed the signature of the expansion of this shell with a velocity of at least 10 km/s. The supernova remnant is located in the vicinity of the densest region of the HI shell (see also Lozinskaya et al., 2003.)

The presence of this shell supports the scenario where supernova exploded inside a cavern surrounded by a dense shell and the expanding remnant collided with the wall of the shell. We proposed this model in Paper I to explain the peculiar nature of the SNR, which combines the properties of a young and old object, being simultaneously bright both in the optical and x-ray domains.

The collision with this outer shell also helps us to understand the peculiar morphology of the SNR. The optical nebula exhibits a well-defined increase of brightness toward the center, which is typical of plerions. At the same time, the radio spectrum ($\alpha = -0.6$ according to Paper I, see also Dickel et al., 1985)) is typical of shell-type SNRs. The elongated crescent-shaped morphology is due to the fact that at optical wavelengths we observe only the brightest sector of the shell-shaped remnant in the dense matter of the outer HI shell. The offset of the center of the distribution of the velocity of the bright component of the H α line with respect to the brightness distribution center, which is evident in Fig. 1, indicates that the bright sector of the supernova remnant is tilted with respect to the sky plane.

It goes without saying that this is a model explains the data provided by the available observations of the SNR S8 . HST observations are needed to thoroughly understand the nature of this extremely interesting object.

5 Conclusions

We measured for the first time the expansion velocity of the bright S8 nebula, which is the only supernova remnant in the dwarf Irr galaxy IC1613. We revealed an HI shell at whose inner boundary the SNR resides. This result supports the scenario proposed in our earlier paper (Lozinskaya et al., 1998) to explain the peculiar nature of the SNR with the supernova exploding inside a cavern surrounded by a dense shell and the supernova remnant then interacting with the wall of the shell.

Acknowledgments We are grateful to A.V.Moiseev for performing observations with the 6-m telescope and valuable discussion. This work was supported by the Russian Foundation for Basic Research (project No. 07-02-00227) and is based on the observational material obtained with the 6-m telescope of the Special Astrophysical Observatory of the Russian Academy of Sciences funded by the Ministry of Science of the Russian Federation (registration number 01-43). The application for 21-line observations of IC 1613 with

NRAO VLA was submitted by E.Wilcots. The National Radio Astronomy Observatory is a facility of the National Science Foundation operated under cooperative agreement by Associated Universities, Inc.

FIGURE CAPTIONS

Fig. 1a - Top – $H\alpha$ image of the S8 supernova remnant superimposed onto the velocity field in the same line (shown by contours). The flux scale in $\text{erg}/(\text{s cm}^2 \text{ \AA})$ is given on the right. Bottom – $H\alpha$ -line velocity field of the remnant superimposed onto the image taken in the same line (shown by contours). The velocity scale (km/s) is given on the right.

Fig. 1b - Velocity field of the supernova remnant in various lines superimposed onto the $H\alpha$ line image (shown by contours). The velocity scale (km/s) is shown on the right of each image.

Fig. 2 - Examples of the decomposition of the $H\alpha$ line into two Gaussians based on MPFS observations. The arrows indicate the regions of the SNR for which the decomposition is made.

Fig. 3 - Same as Fig. 2, but based on FPI observations.

Fig. 4a - "Position-velocity" diagrams for two components of the $H\alpha$ line made in the direction parallel to the major axis of the SNR based on MPFS (left) and FPI (right) observations. The location of the scans on the image of the nebula is shown at the top and the velocities of the two line components along these scans are given by different symbols at the bottom.

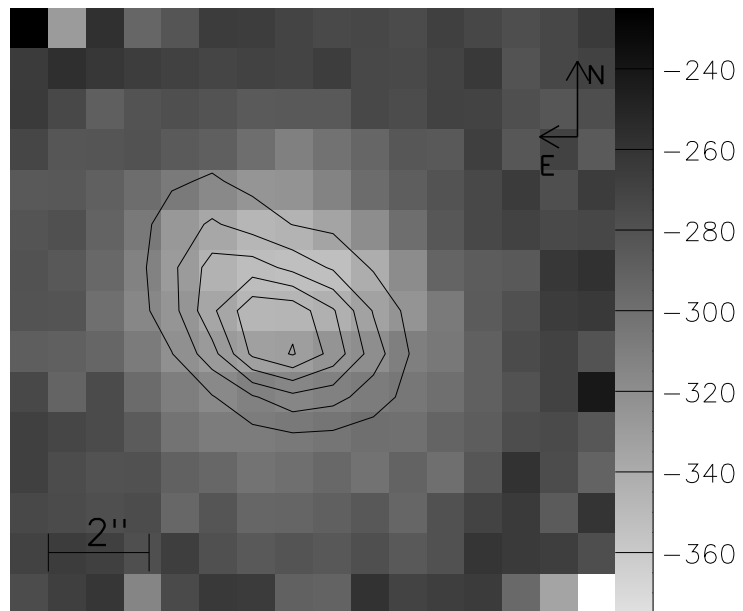
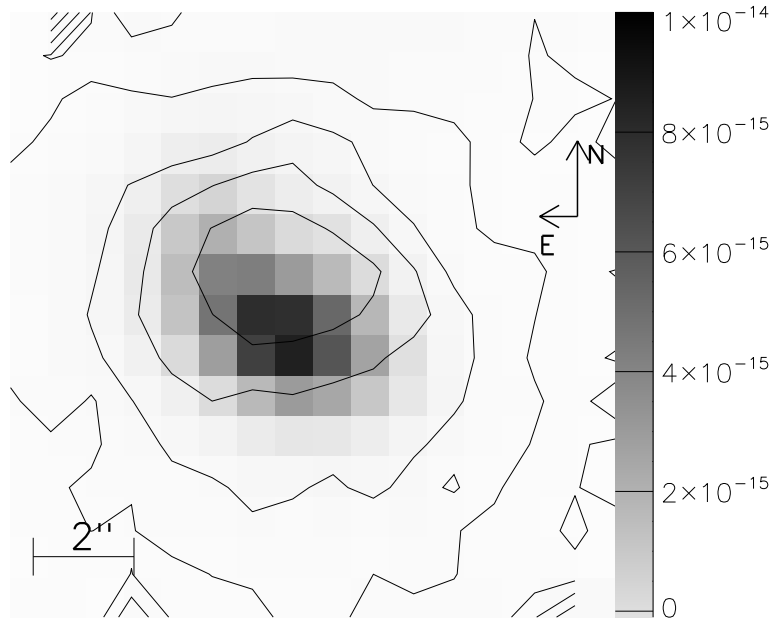
Fig. 4b - Same as Fig. 4a, but for the minor axis of the SNR based on FPI observations.

Fig. 5 - Top – The 21-cm line image of the galaxy superimposed on $H\alpha$ line brightness contours. The thick arrow indicates the S8 supernova remnant. Arrows 1, 2, and 3 indicate the locations of the three scans used to construct the 21-cm line P/V diagrams shown below. The vertical lines indicate the position of the SNR on the P/V diagrams.

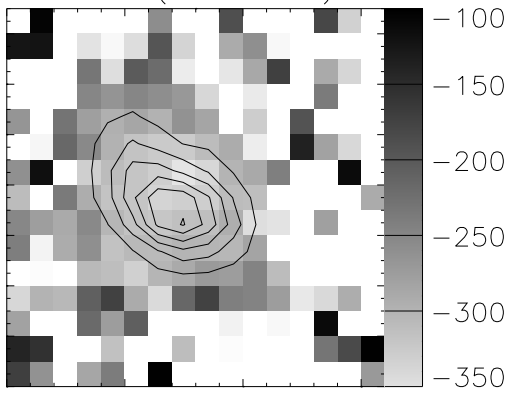
References

- [1] Dickel, J. R., d’Odorico, S., and Silverman, A., *Astron.J.*, **30**, 414 (1985)
- [2] Lozinskaya T.A., Silchenko O.K., Helfand D.J., Goss M.W.), *Astron.J.*, **116**, 2328 (1998) Paper (I)
- [3] Lozinskaya T.A., Moiseev A.V. Afanas’ev V.L., Wilcots E., Goss V.M., *Astron. Zh.*, **78**, 485 (2001)
- [4] Lozinskaya T.A., *Astron. Astroph. Trans.*, v.21, **No 4-6**, p.223-229 (2002).
- [5] Lozinskaya T.A., Moiseev A.V., Podorvanyuk N.Yu., *Pis’ma Astron. Zh.*, **29**, No 2, c. 95-110 (2003); astro-ph/0301214
- [6] Lake G., Skillman E.D., *Astron.J.*, **98**, 1274 (1989)
- [7] Meaburn, J., Clayton, C.A., and Whitehead, M.G.), *MNRAS*, **235**, 479 (1988)
- [8] Moiseev, 2002, Preprint of the Special Astrophysical Observatory of the Russian Academy of Sciences, No. 166, 1 (2002).
- [9] Rosado M., Valdez-Gutierrez M., Georgiev L. et al., *Astron.J.*, **122**, 194 (2001)

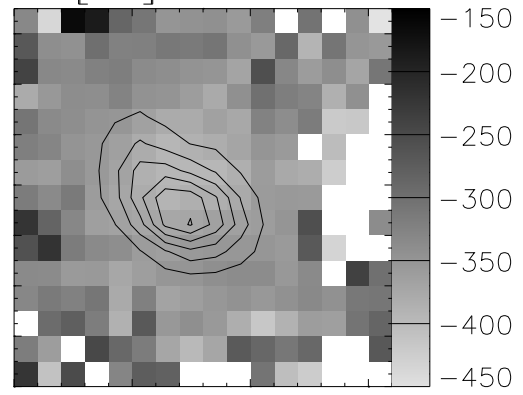
- [10] Silich S., Lozinskaya T., Moiseev A., Podorvanyuk N., Rosado M., Borissova J., Valdez-Gutierrez M, *Astron. Astrophys.*, **448**, 123-131 (2006)
- [11] Sandage A., *Astrophys. J.*, **166**, 13 (1971)
- [12] Freedman, W.L., *Astrophys. J.*, **326**, 691 (1988)



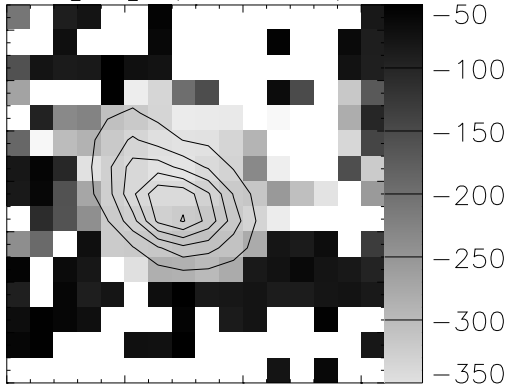
HeI (5876 A)



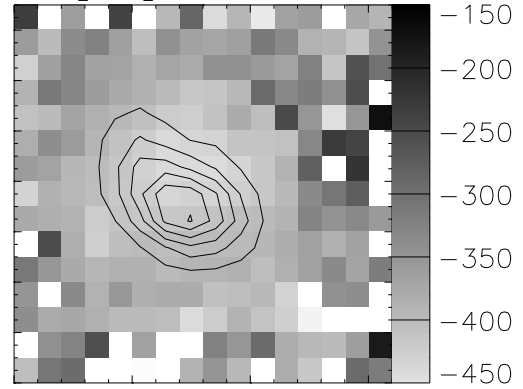
[SII] 6717 A



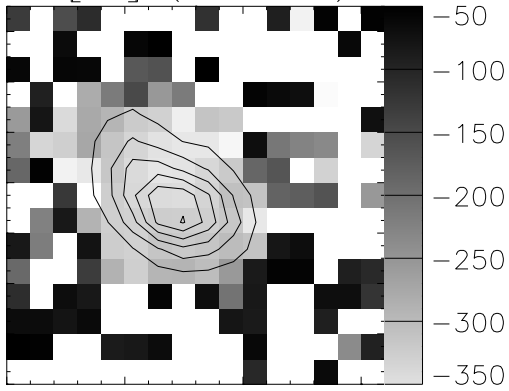
[OI] (6300 A)



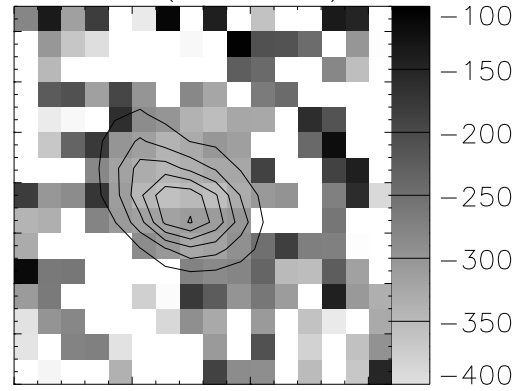
[SII] 6733 A



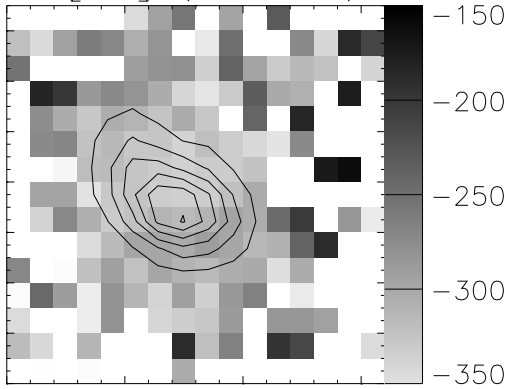
[OI] (6364 A)



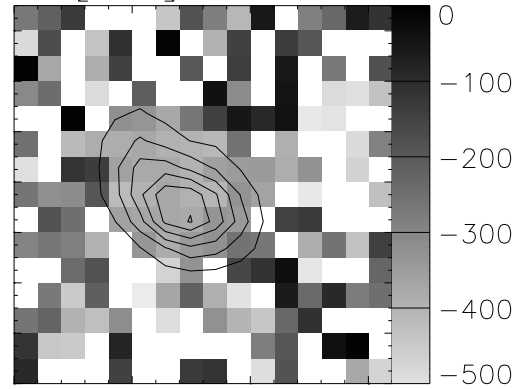
HeI (7065 A)



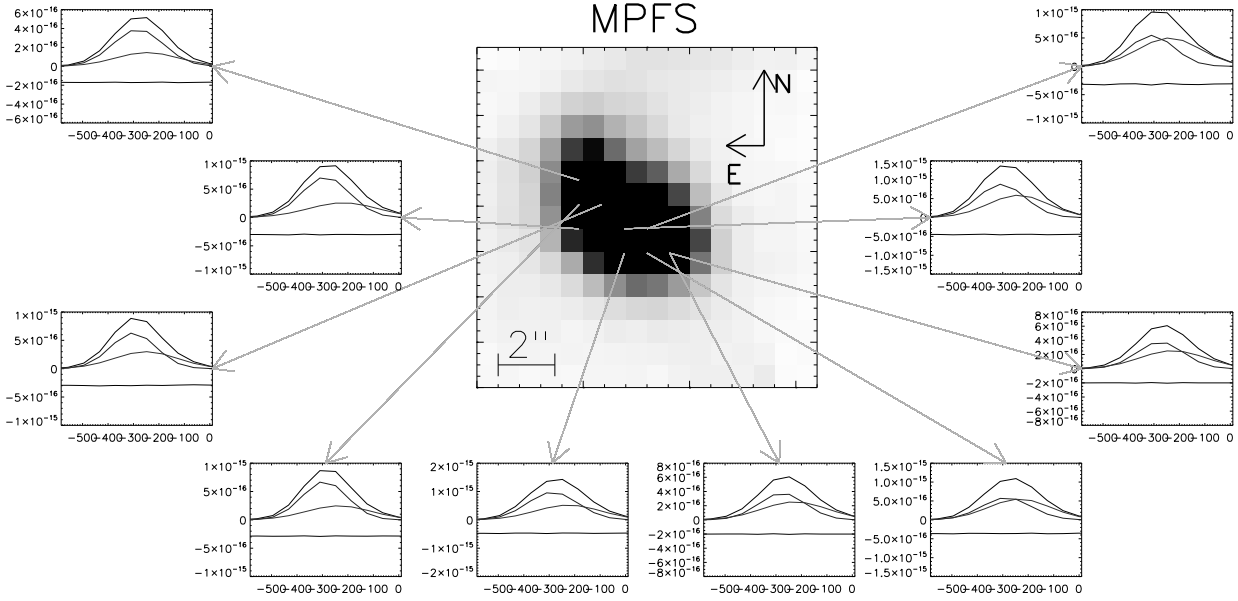
[NII] (6583 A)

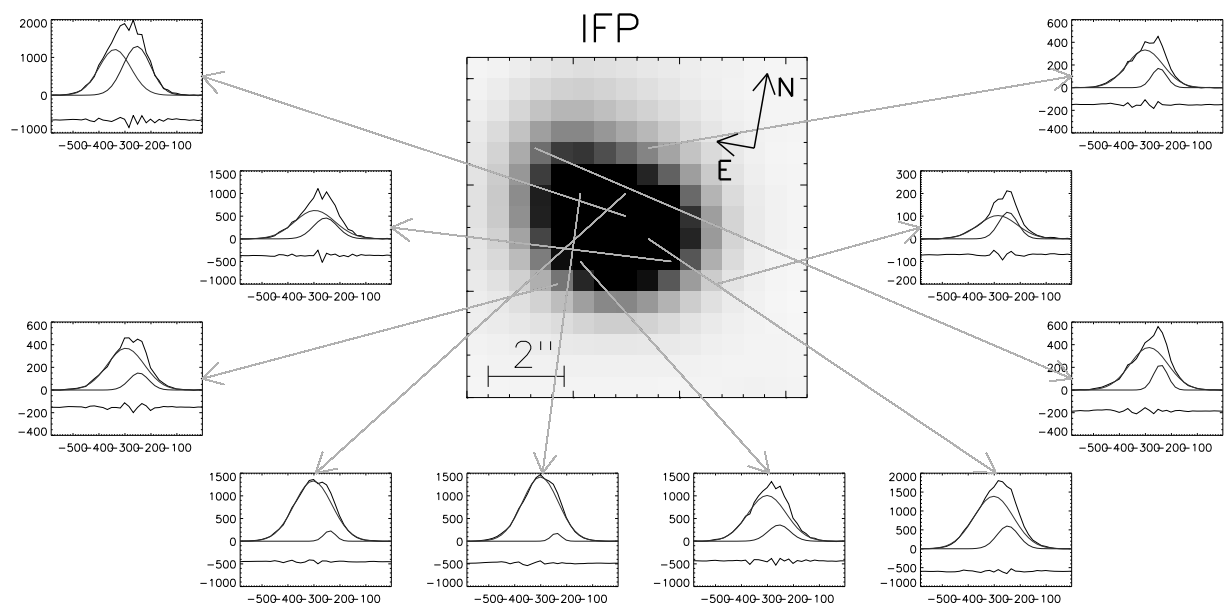


[FeII] 7155 A

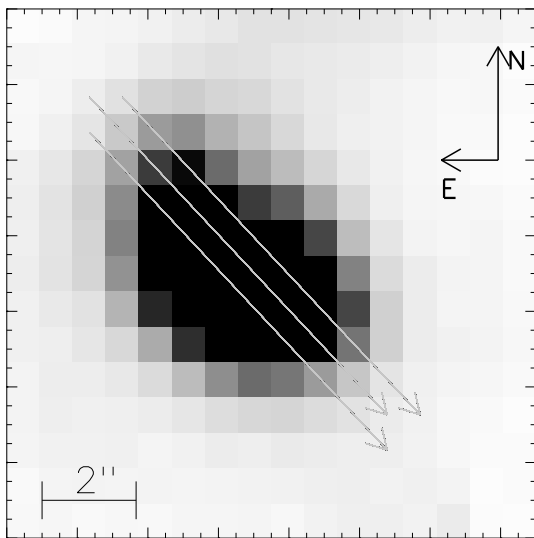


MPFS

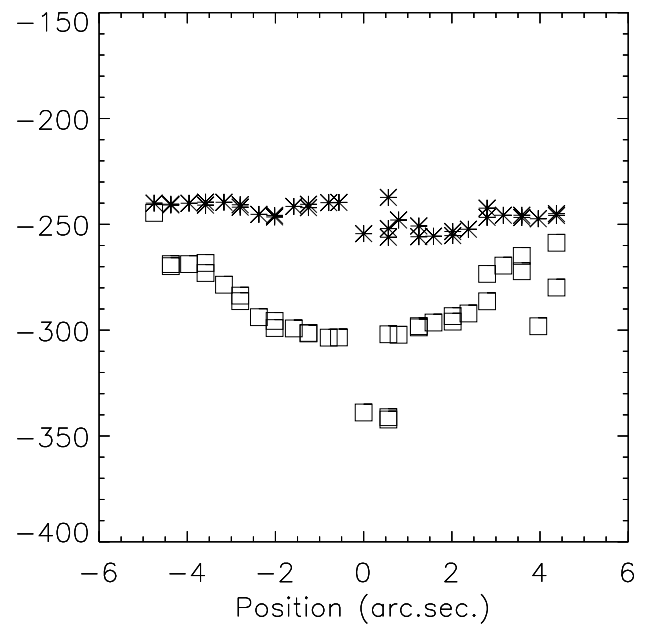
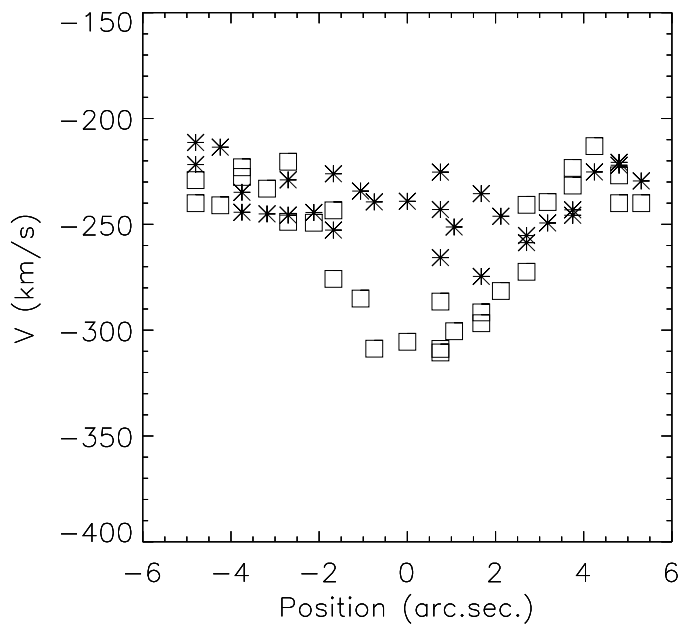
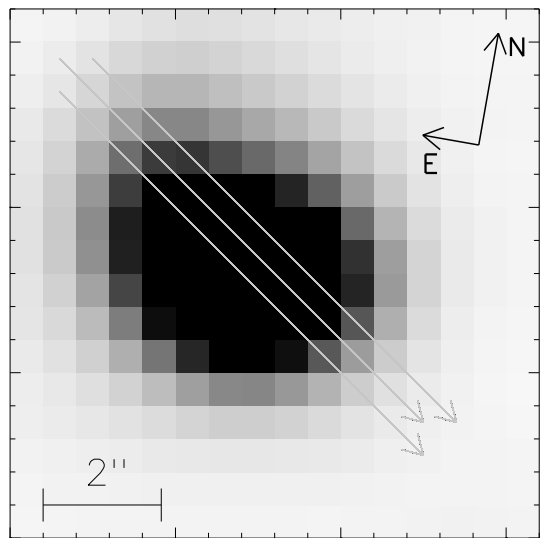




MPFS



IFP



IFP

